

# Gravity-free hydraulic jumps and metal femtocups

Rama Govindarajan<sup>1,\*</sup>, Manikandan Mathur<sup>1,†</sup>, Ratul DasGupta<sup>1</sup>,  
N.R. Selvi<sup>2</sup>, Neena Susan John<sup>2</sup> and G.U. Kulkarni<sup>2,\*</sup>

1. *Engineering Mechanics Unit and 2. Chemistry and Physics of Materials Unit and DST Unit on Nanoscience, Jawaharlal Nehru Centre for Advanced Scientific Research, Jakkur, Bangalore 560064, India.*

† *currently at Dept. of Mechanical Engineering, MIT, Cambridge, MA 02139, USA.*

(Dated: April 9, 2018)

Hydraulic jumps created by gravity are seen every day in the kitchen sink. We show that at small scales a circular hydraulic jump can be created in the absence of gravity, by surface tension. The theory is motivated by our experimental finding of a height discontinuity in spreading submicron molten metal droplets created by pulsed-laser ablation. By careful control of initial conditions, we show that this leads to solid femtolitre cups of gold, silver, copper, niobium and tin.

PACS numbers: 47.61.-k, 47.85.Dh, 47.55.nd

It has long been observed that water flowing horizontally can display a discontinuity in height [1, 2, 3]. This is the *hydraulic jump*, seen for example when water from a faucet impinges on the kitchen sink and spreads outwards. Gravity is a key ingredient in these well-understood *large-scale* hydraulic jumps, as discussed briefly below. In this Letter we show, remarkably, that the shallow water equations support solutions for a *gravity-free* hydraulic jump. The driver here is surface tension at the liquid-air (or liquid-vacuum) interface, and jumps may be expected to occur when relevant length scales are submicron. Our theoretical study was prompted by careful experiments showing that molten metal droplets impinging on a solid substrate display such a jump, solidifying into cup-shaped containers of femtolitre capacity. The droplets are created by laser-ablation of a solid metal target. Femtocups made of different metals on various substrates are formed under carefully maintained conditions of laser energy and substrate temperature. Outside this narrow range of parameters we find what one would normally expect: the droplets solidify into lump-shaped structures on the substrate. The ability to make, and subsequently leach out, femtocups at will has potential applications ranging from nanoscale synthetic chemistry to single cell biology.

Before describing the experiments and the femtocups, we discuss what causes a gravity-free hydraulic jump. Consider a steady axisymmetric jet of fluid of radius  $a$  impinging on a solid plate placed normal to the flow. The density of the surrounding medium is assumed to be negligible. The fluid then spreads radially outwards within a relatively thin film. The dynamics within the film is described by the axisymmetric shallow-water equation [4, 5, 6]

$$u \frac{\partial u}{\partial r} + w \frac{\partial u}{\partial z} = \nu \frac{\partial^2 u}{\partial z^2} - gh' + \frac{\sigma}{\rho} \frac{d}{dr} \left[ \frac{\nabla^2 h + (h'^3/r)}{(1 + h'^2)^{3/2}} \right], \quad (1)$$

where  $r$  and  $z$  are the radial coordinate and the coordinate perpendicular to the solid wall respectively, with origin on the solid surface at the centre of the impinging jet. The respective velocity components are  $u$  and  $w$ . The total height  $h$  of the fluid above the surface is

a function of  $r$ , and a prime thus denotes a derivative with respect to  $r$ . The parameters in the problem are the acceleration due to gravity,  $g$ , the surface tension coefficient,  $\sigma$  for the liquid-air or liquid vacuum interface, and the density  $\rho$  and the kinematic viscosity  $\nu$  of the impinging fluid. For incompressible axisymmetric flow the equation of continuity, in differential and in global form, reads

$$\frac{\partial u}{\partial r} + \frac{u}{r} + \frac{\partial w}{\partial z} = 0 \quad \text{and} \quad 2\pi \int_0^{h(r)} ru(r, z) dz = Q, \quad (2)$$

where  $Q = \pi a^2 u_j$  is the steady inlet volumetric flow rate. A characteristic inlet jet velocity  $u_j$  is thus defined. It is reasonable to assume [3] a parabolic shape in  $z$  for the radial velocity

$$u(r, z) = \zeta(r)(z^2 - 2h(r)z) \quad (3)$$

satisfying the no-slip condition at the wall ( $z = 0$ ) and the zero shear stress condition at the free surface ( $z = h$ ). The analysis does not hinge on this assumption; any reasonable profile shape will give qualitatively the same results. Using Eq. (2) and the kinematic condition  $w = Dh/Dt = uh'$  at  $z = h$ , the momentum equation (1) integrated over  $z$  from 0 to  $h$  reduces after some algebra to

$$b \left( \frac{h}{r} + h' \right) = \frac{2r}{R} + \frac{h^3 r^2}{F} h' - \frac{r^2 h^3}{W} \frac{d}{dr} \left[ \frac{\nabla^2 h + (h'^3/r)}{(1 + h'^2)^{3/2}} \right], \quad (4)$$

where all lengths are scaled by  $a$ , and the  $O(1)$  positive constant  $b = 2/5$  for a parabolic profile. The left-hand side of (4) represents inertia, and the three terms on the right hand side appear due to viscosity, gravity and surface tension respectively. The relative importance of the inertial term to each of these is quantified respectively by the Reynolds number  $R \equiv u_j a / \nu$ , the Froude number  $F \equiv u_j^2 / (ga)$ , and the Weber number  $W \equiv \rho u_j^2 a / \sigma$ . In large-scale flows surface tension has been shown [5] only to make a small correction to the location of the jump, so the last term is unimportant. This is to be expected, since  $F$  in the kitchen sink is of order unity, while

$W \sim 10 - 100$ . In contrast, consider  $u_j \sim 10$  m/s and  $a \sim 10^{-7}$  m, so  $F \sim 10^8$  and  $W \sim 10^{-2}$ . Here surface tension determines whether and where a jump will occur, whereas it is the *gravity* term that may be dropped entirely from the equation.

In general, a jump occurs if the pressure gradient becomes increasingly adverse as the flow proceeds downstream, and attains a magnitude large enough to counter the relevant inertial effects. The adverse pressure gradient may be created by gravity, or surface tension, or both. With gravity alone, Eq. (4) reduces to

$$h' = \frac{2r/R - bh/r}{b - h^3 r^2 / F}. \quad (5)$$

It is seen that if  $F$  is finite and  $h^3 r^2$  is an increasing function of  $r$ , the denominator will go to zero at some  $r$ , i.e., a jump will occur in the framework of the shallow-water equations [1, 2, 4, 5]. However, its precise location may not coincide with this estimate [4], and in a given experiment the radial extent available may be too small, or the inertia too low, for a jump to occur. Decreasing gravity has been shown to shift the jump location downstream [10], consistent with Eq. (5). Now considering surface tension alone, a crude prediction of the existence of a jump may be made by assuming the height upstream to be slowly varying in  $r$ , i.e.,  $h' \ll 1$ , and thus setting  $h'' = h''' = 0$ . We may then rewrite Eq. (4) as

$$h' \simeq \frac{2r/R - bh/r}{b - h^3/W}. \quad (6)$$

A jump is now possible if  $h$  is an increasing function of  $r$ , which is a more stringent requirement than in the case of gravity. Note that the second term in the denominator appears due to *radial* spreading, i.e., surface tension alone cannot give rise to a one-dimensional jump like a tidal bore.

We now solve Eq. (4) as an initial value problem beginning at some location  $r_i$  and marching downstream. A fourth-order Runge-Kutta algorithm is used. An initial radius  $r_i$  somewhat larger than  $a$  is chosen, where it is assumed that a parabolic profile has been attained. The initial conditions in  $h$  and its derivatives are not known exactly for this complicated problem, and numerical studies are being done to understand the flow in this vicinity. We have, however, repeated the computations with a variety of initial height profiles, and a range  $1.2 < r_i < 5$  and  $0.1 < h < 1$ , and the results do not change qualitatively. Typical solutions are shown in figure 1. At a particular radial location  $r = r_j$ , there is a singularity in the height of the fluid layer. Note that as we approach  $r_j$  the shallow water equations are no longer valid, even approximately, so the present analysis cannot tell us anything about the actual shape close to or after the jump. The dependence of the jump location on the inlet jet velocity  $u_j$  is not monotonic, as seen from figure 2a. Here the Reynolds number  $R$  is varied by changing  $u_j$ , with other quantities as in figure 1, so the Weber number increases as  $R^2$ , from  $3 \times 10^{-9}$  to 90. For very low  $R$  or

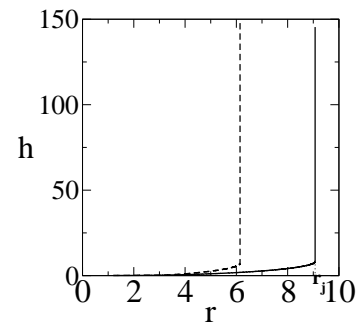


FIG. 1: Typical solutions of Eq. (4), with  $F = \infty$ , containing a singularity at  $r = r_j$ . For demonstration, liquid properties are taken as those of molten silver ( $\rho = 5000$  kg m $^{-3}$ ,  $\nu = 10^{-6}$  m $^2$ /s and  $\sigma = 0.9$  N m $^{-1}$ ) and  $a = 5$   $\mu$ m. Solid line:  $u_j = 5$  cm/s; dashed line:  $u_j = 80$  m/s. Values for molten tin show similar behavior.

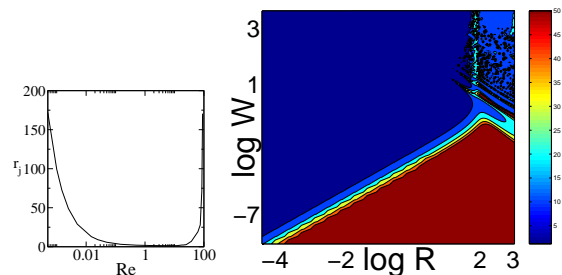


FIG. 2: (a) The location  $r_j$  of the singularity as a function of the inlet jet radius, expressed here in terms of the Reynolds number. For  $R = 0.01 - 90$  ( $u_j = 0.02 - 180$  m/s for the case considered) the jump radius is of the order of a few microns, as observed in the experiment described below. (b) Contour plot of jump location in the  $R - W$  plane.

very high  $W$ , jumps are unlikely to form within the available radius, i.e., inertia and surface tension must be in the right balance. The Reynolds and Weber numbers are now varied independent of each other (figure 2b). In the region shown in red  $r_j > 60$  so jumps are not predicted. (A higher cut-off does not change answers qualitatively.) Blue color indicates  $r_j \sim r_i$ , this region merits numerical investigation. Gravity-free hydraulic jumps may be expected in the region shown by intermediate color, seen as a relatively narrow linear patch when  $R < 100$ . Here the jump location depends only on the ratio  $W/R$ . For a given  $W$ , jumps exist for over an order of magnitude variation in  $R$ . At  $R > 100$ , undular jumps are seen, which are being investigated further.

We turn now to our experiments, which show a height discontinuity in spreading drops of molten metal. Since the experimental flow is transient in nature, a detailed comparison with the theoretical results is not possible, but the jump radius is in the right range. At larger scales hydraulic jumps are known to occur even when the incoming flow is in droplets rather than jets [11]. A Q-switched frequency tripled Nd:YAG laser ( $\lambda = 355$

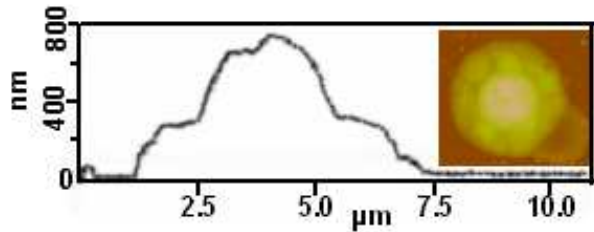


FIG. 3: AFM image (right) and height profile (left) of a silver blob on silicon substrate kept at room temperature.

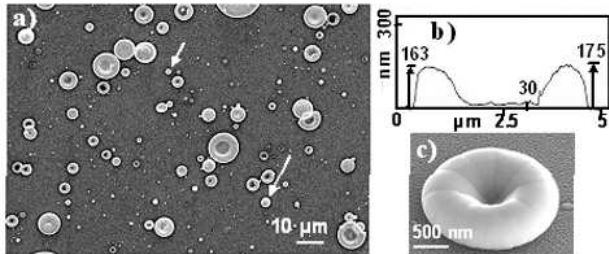


FIG. 4: Microscopy analysis of metal cups (a) SEM image of femtocups of silver on a silicon substrate obtained at  $E_p = 100$  mJ/pulse and  $T_s = 1173$  K. A few blobs do exist, as indicated by arrows. (b) Typical height profile of a femtocup from AFM analysis. (c) Tilted field emission SEM image of a tin femtocup on silicon.

nm, repetitive frequency, 10 Hz) is focused with pulse energy  $E_p$  on a rotating metal disc in a vacuum chamber ( $10^{-7}$  torr) and the resultant plume received at a distance of 4 cm on a clean vertical substrate held at a temperature  $T_s$ , for a duration of 20 min [7]. The resulting metallic structures on the substrate are studied by scanning electron microscopy (SEM), atomic force microscopy (AFM) and energy dispersive X-ray analysis (EDAX). Over most of the range of  $E_p$  and  $T_s$ , we expect, and obtain, ill-shaped blobs of solidified metals, see figure 3. However, for a small range of these parameters, there is a strong preference to form cup-like structures of outer diameters  $\sim 300$  nm to  $10 \mu\text{m}$ , with side walls  $\sim 100$  nm high, and capacity  $\sim 1$  fL (fig. 4). The jump diameter is usually about half the total diameter. Height profiles associated with atomic force micrographs (figure 4b) as well as EDAX spectra (not shown) [7] confirm that the central region is raised from the substrate and contains metal. Interestingly, pulsed-laser ablation has been used extensively to produce a variety of structures [8], but femtocups have not been reported before, although we notice stray instances of similar structures in other studies [9].

This surprising femtocup structure is consistent with the proposed dynamics: of a droplet spreading out thinly initially and then undergoing a height discontinuity. We obtain femtocups of gold, silver, copper, tin and niobium of repeatable statistics on glass, silicon and graphite

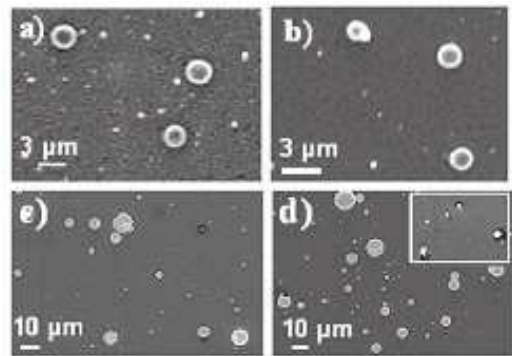


FIG. 5: SEM images with different metals, laser energy and substrate temperature. (a) Cu femtocups on Si.  $E_p=100$  mJ/pulse,  $T_s = 300$  K; (b) Nb on Si,  $E_p=100$  mJ/pulse,  $T_s = 1273$  K; (c) Ag on Si,  $E_p = 60$  mJ/pulse. The number density of well-formed cups is lower. (d) Ag on Si,  $E_p = 100$  mJ/pulse,  $T_s = 773$  K much less than  $T_m = 1234$  K. The cups are not well-formed. Inset,  $T_s = 1273$  K  $> T_m$ . Only patches are observed.

(HOPG), see examples in figure 5a and b, and later in figure 7. The solid surface being vertical and the length scales small mean that the effect of gravity is negligible. Inertia on the other hand is considerable, since velocities are high. We do not have a direct estimate of  $u_j$ , but we may estimate it from earlier measurements in many similar experiments [12] to range between 1 m/s to 100 m/s. Also, the range of  $R$  and  $W$  over which a surface-tension driven hydraulic jump occurs translates to a particular range of  $E_p$ , since laser fluence determines scales and speeds in the incoming jet, compare figures 4a and 5c. While the substrate is hotter than the metal's melting point  $T_m$ , the cup may form initially but cannot solidify and liquid flows back into the cup, so the final object is as seen in the inset of figure 5d. With  $T_s$  far below  $T_m$  the tendency to form cups is much reduced (figure 5d, probably because solidification is too rapid for flow to be completed). Optimal conditions are thus  $E_p$  ( $\sim 100$  mJ/pulse for silver) and  $T_s$  close to but below  $T_m$ . Outside the correct range, blobs form rather than cups.

That the jump is directly related to droplet dynamics is confirmed by varying the substrate orientation with respect to the incoming jet (see schematic in Fig. 6). As  $\theta$ , the inclination of the substrate away from the normal, is increased, the structures become increasingly elliptical, especially beyond  $40^\circ$ , in accordance with the azimuthal variation of  $R$  and  $W$ .

Since the experiment includes additional complexity in the form of solidification, we estimate relative time-scales of jump formation  $t_j$  and solidification of a droplet  $t_c$ . For the experimental values of substrate thickness,  $t_c$  ranges from  $\sim 3 \times 10^{-4}$  s on silicon to  $\sim 10^{-2}$  s on glass (taking into consideration conduction, radiation and latent heat), while  $t_j \sim r_j/u_j \sim 10^{-6}$  s or less. Contact-line freezing can give rise to an increase in height in the vicinity, typically amounting to a small percentage of the height

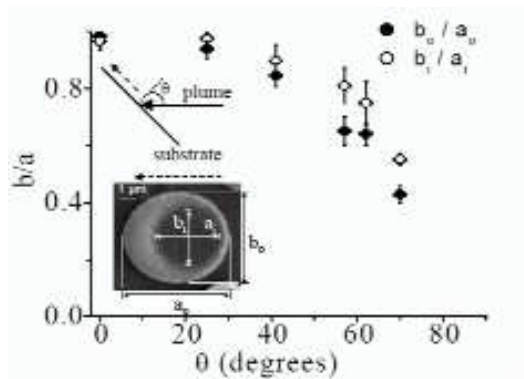


FIG. 6: Elliptical femtocups with inclined jets. Inset: Sample SEM image of tin obtained at  $\theta = 40 \pm 1.5^\circ$ , defining  $a$  and  $b$ . The ratio  $b/a$  increases with  $\theta$ , each data point is an average on several cups. The major axis lies along the direction of maximum flow (dashed arrows).

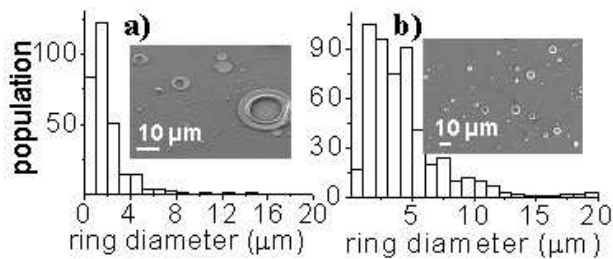


FIG. 7: Histograms and SEM images of tin femtocups on (a) glass and (b) silicon, deposited simultaneously.

in the central region. Contrast this to our jump where the height at the rim is several-fold larger than that in the central region. In spite of this, and the disparity in time scales, we cannot rule out a role for local freezing

at the contact line [13]. We do notice a dependence on the substrate of the size distribution of femtocups (figure 7) and also some visual differences in the shape of the femtocup. Our ongoing numerical study, including a non-uniform temperature profile and its effects, is therefore aimed at a better representation of the experiments. Also being addressed are the experimental finding of radial striations in the femtocups under certain conditions, and the theoretical finding of undular hydraulic jumps (similar to [14] in other conditions) when  $R$  is greater than about  $25/W$  (figure 8).

In summary, for the first time, a hydraulic jump solely driven by surface tension is shown to occur. Experimentally we show evidence for such jumps in submicron high inertia droplets of molten metals spreading radially outwards on a substrate. The detailed shape in the vicinity of the jump and the transient problem including the solidification process is being studied numerically.

We are grateful to Prof. G Homsy, Prof. CNR Rao and Prof. R Narasimha for useful discussions. RG and

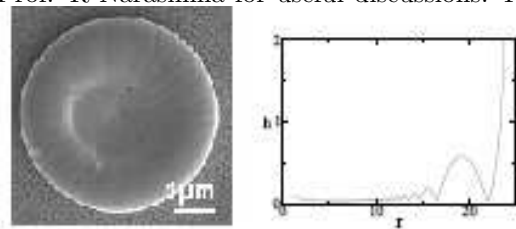


FIG. 8: (a) Striations in the structure. (b) An undular hydraulic jump at  $R = 5000$ ,  $W = 0.005$ .

NSJ acknowledge support from DRDO (India) and CSIR (India) respectively.

\* To whom correspondence should be addressed, rama@jncasr.ac.in, kulkarni@jncasr.ac.in

- 
- [1] L Rayleigh, *Proc. R. Soc. Lond. A*, **90**, 324-328 (1914).  
 [2] E.J. Watson, *J. Fluid Mech.* **20**, 481-499 (1964). C. Ellegaard *et al.*, *Nature*, **392**, 767-768 (1998). T. Bohr, V. Putkaradze, & S. Watanabe, *Phys. Rev. Lett.*, **79**, 1038-1041 (1997). S.B. Singha, J.K. Bhattacharjee & A. Rai *Eur. Phys. J. B*, **48**, 417-426 (2005). J.W.M. Bush, J.M.J. Aristoff & A. E. Hosoi, *J. Fluid Mech.*, **558**, 33-52, (2006).  
 [3] I. Tani, *J. Phys. Soc. Japan*, **4**, 212-215, (1949).  
 [4] T. Bohr, P. Dimon & V Putkaradze *J. Fluid Mech.* **254**, 635-648 (1993).  
 [5] J.W.M. Bush & J.M.J. Aristoff, *J. Fluid Mech.* **489**, 229-238 (2003).  
 [6] L.D. Landau & E.M. Lifshitz, *Fluid Mechanics (Course of Theoret. Phys., Vol. 6)*, Pergamon press, U.K., (1987).  
 [7] G.U. Kulkarni *et al.* preprint, NS John, PhD thesis, (2006).  
 [8] M. Terrones, *et al.*, *Nature*, **388**, 52-55 (1997). A. Thess, *et al.*, *Science*, **273**, 483-487 (1996). X. Duan & C.M. Lieber, *Adv. Mater.* **12**, 298-302 (2000). Y. Zhang, K. Suenaga, C. Colliex & S. Iijima, *Science*, **281**, 973-975 (1998). UK Gautam *et al.*, *J. Am. Chem. Soc.*, **127**, 3658-3659 (2005).  
 [9] C.J.K Richardson *et al. Mat. Res. Soc. Symp.* **617**, J7.4.1-J7.4.6 (2000). S.J. Henley, M.N.R. Ashfold & S.R.J. Pearce, *Appl. Surf. Sci.* **217**, 68-77 (2003).  
 [10] C.T. Avedisian & Z Zhao *Proc. R. Soc. Lond. A* 456, 2127-2151 (2000).  
 [11] S. Chandra & C.T. Avedisian *Proc. R. Soc. Lond. A*, 432, 13-41 (1991).  
 [12] D.B. Chrisey & G.K. Hubler *Pulsed Laser Deposition of Thin Films* Wiley, New York (1994) and references therein.  
 [13] S. Schiaffino & A. A. Sonin, *Phys. Fluids* **9**, No. 8, 2227-2233; and 2217-2226 (1997).  
 [14] R.I. Bowles & F.T. Smith, *J. Fluid Mech.*, **242**, 145-168.

H. Steinruck, W. Schneider & W. Grillhofer, *Fluid Dyn. Res.*, **33** 41-55 (2003).